TITLE
On the results of causal optogenetic engram manipulations

RUNNING TITLE: Optogenetic stimulation elicits endogenous patterns of neural activity.

Claudia Jou[a], José R. Hurtado[b], Simon Carrillo-Segura[b,c], Eun Hye Park[b], André A. Fenton[b,d,#]

[a]Graduate Center, Hunter College, City University of New York, New York, NY 10016

[b]Center for Neural Science, New York University, New York, NY 10003

[c]Graduate Program in Mechanical and Aerospace Engineering, Tandon School of Engineering, New York University, Brooklyn, NY 11201

[d]Neuroscience Institute at the New York University Langone Medical Center, New York, NY 10016

Author Contributions: CJ, and AAF designed the research, CJ, JH, and EHP performed the research, CJ and SS-C analyzed the data and AAF and CJ wrote the paper.

[#]Correspondence should be addressed to:

André A. Fenton

Center for Neural Science

New York University

4 Washington Place

New York, NY 10003

SUMMARY

Cellular-resolution manipulation technologies like optogenetics enable so-called causal engram-cell experiments in which learning-activated neurons are tagged with a light-responsive protein (opsin) such that subsequent photostimulation elicits memory behavior. The opsin-tagged neurons are considered key neural circuit elements with photostimulation demonstrating their sufficiency for memory expression. Can the sufficiency interpretation be correct if the brain is a complex dynamical system with adaptive, non-linear, and homeostatic interactions? We find that during photostimulation of place avoidance memory-tagged neurons, mouse CA1 hippocampus activity maintains intrinsic ensemble discharge relationships and the low-dimensional manifold organization of the population dynamics. Although the photostimulation causes spatially-precise conditioned avoidance, such manipulations, are better interpreted as eliciting the endogenous population dynamics of a complex system, rather than the causal demonstration of neural circuit function.

The mammalian brain is characterized by adaptive, non-linear responses and interactions, with inertial history that we sometimes call memory, though they can be generated locally, independently of experience [1,2]. As is typical of a complex system, many neural phenomena are emergent in that they are only observed as a property of the whole system, without manifesting at the level of the components [3,4]. The brain is also composed of a series of interacting neural circuits, the operations of which tend to be specialized for particular functions. The neuronal elements of functionally distinct circuits are typically anatomically interspersed, creating a basic challenge for how to experimentally define and investigate functionally distinct neural circuits. Localized manipulations that nonetheless affect multiple functionally distinct circuits can be expected to produce difficult to predict outcomes [5,6]. One of the challenges of experimental neuroscience is in the tension between interpreting experimental outcomes as the property of a

complex system, or alternatively, interpreting outcomes as the result of an off-target circuit manipulation.

Optogenetics, chemogenetics, and other neuron-specific manipulations have been revolutionary by enabling so-called causal experiments that selectively manipulate specific neurons to evaluate their hypothesized function. Despite enabling an unprecedented ability to identify functional neural circuits by the effective connections amongst neurons, it remains unclear how to correctly interpret the results of these precise manipulations of a system with adaptive, non-linear, and inertial interactions (Fig. 1A), in particular because Ashby's law of requisite variety requires an effective controller to possess at least as many states as the system to be controlled [7]. Accordingly, Ashby-like "homeostatic" hypotheses predict photostimulation will elicit familiar network-wide intrinsic homeostatic responses, whereas "causal" hypotheses predict novel stimulus-controlled network responses.

We began by using a heuristic neural network model of excitatory and inhibitory cells in which the excitatory cells learn to distinguish the locations along a circular track with location-specific firing because of spike timing-dependent plasticity (STDP) rules (Levy et al., 2021; Fig. 1B). After sufficient training, excitatory photostimulation was simulated by periodically activating a random subset of the excitatory cells during exploration of the track. Consistent with homeostasis [7], but potentially contradicting observations in key causal experiments [8,9], stimulation of up to 30% of the model cells only rarely (20%) disturbed location-specificity. Even stimulating 40% or more sometimes did not disturb location-specificity (Fig. 1C); the results were similar with the STDP rules off during stimulation (Fig. 1C, S1), motivating us to investigate whether or not (causal) stimulus-induced or (homeostatic) intrinsic network patterns are elicited by optogenetic stimulation of neuron in the intact mouse brain.

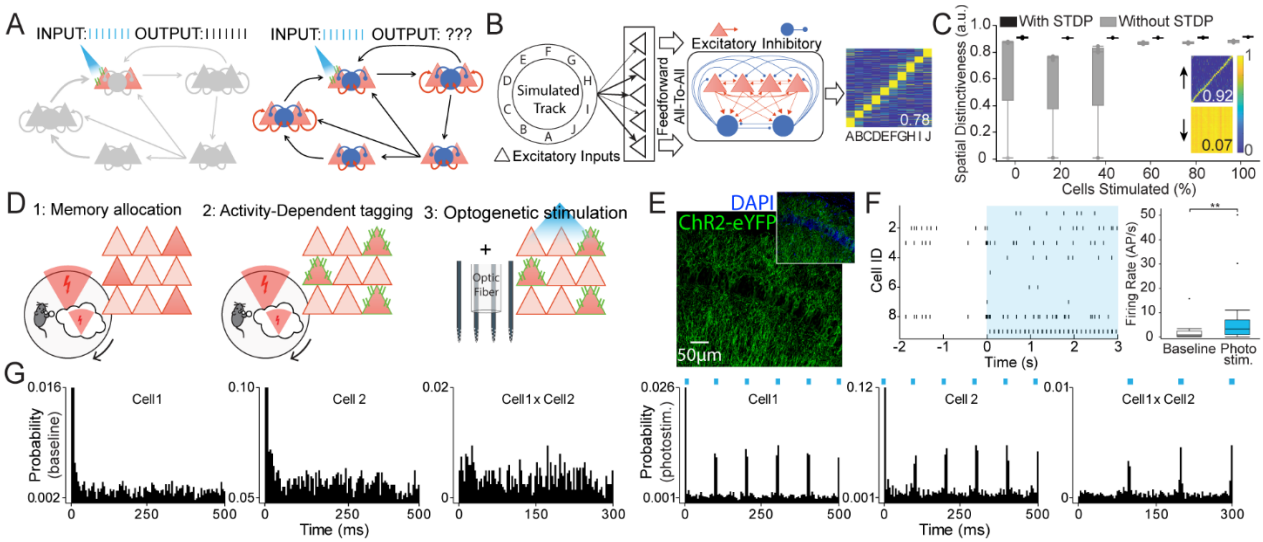

Figure 1. Optogenetic tagging and stimulation of neural circuits *in vivo*. A) Optogenetically-tagged neurons might respond predictably to photostimulation as if (left) network effects were minimal or (right) respond unpredictably due to strong network effects. B) Neural network architecture illustrating that the 10 locations (A-J) of a ring-shaped environment are randomly mapped to "sensory" units which in turn project to a network of 500 excitatory (E) and 50 inhibitory (I) units that are interconnected by activity dependent STDP-modifiable E-E, E-I, and I-I connections. With experience the E units acquire location-specific activity patterns, here shown as a matrix with x-axis: locations, y-axis: cell identity sorted by location of peak activity, and average activity indicated by the blue-yellow color scale. The location-specificity is quantified as spatial distinctiveness C) Spatial distinctiveness is minimally changed by periodically stimulating a random proportion of E cells, illustrating that optogenetic stimulation could have minimal effects on network activity. D) Schematic experimental design and E) immunofluorescence identifying memory-tagged CA1 neurons. Under urethane anesthesia, electrophysiological effects of 10-Hz photostimulation of memory-tagged CA1 principal cells CA1 ensemble discharge F) illustrated as a raster and G) as auto- and cross-correlograms of two neurons during baseline (left) and photostimulation (right). *p<0.05, **p<0.01, ***p<0.001.

During the expression of a long-term active place avoidance memory, the mostly excitatory neurons that (strongly) expressed the immediate early gene *Arc* were indelibly tagged with an enhanced yellow fluorescent protein (eYFP) and channelrhodopsin (ChR2) fusion protein, consequent to transient Cre-mediated recombination Fig. 1D,E; [10,11,12]. Weeks later, under urethane anesthesia, the ChR2-tagged hippocampal CA1 neurons were activated by 10-Hz light pulses that increased firing, as predicted by causal hypotheses (Fig. 1F). Both auto- and cross-correlograms show 10-Hz 473-nm photostimulated neuronal activation (Fig. 1G).

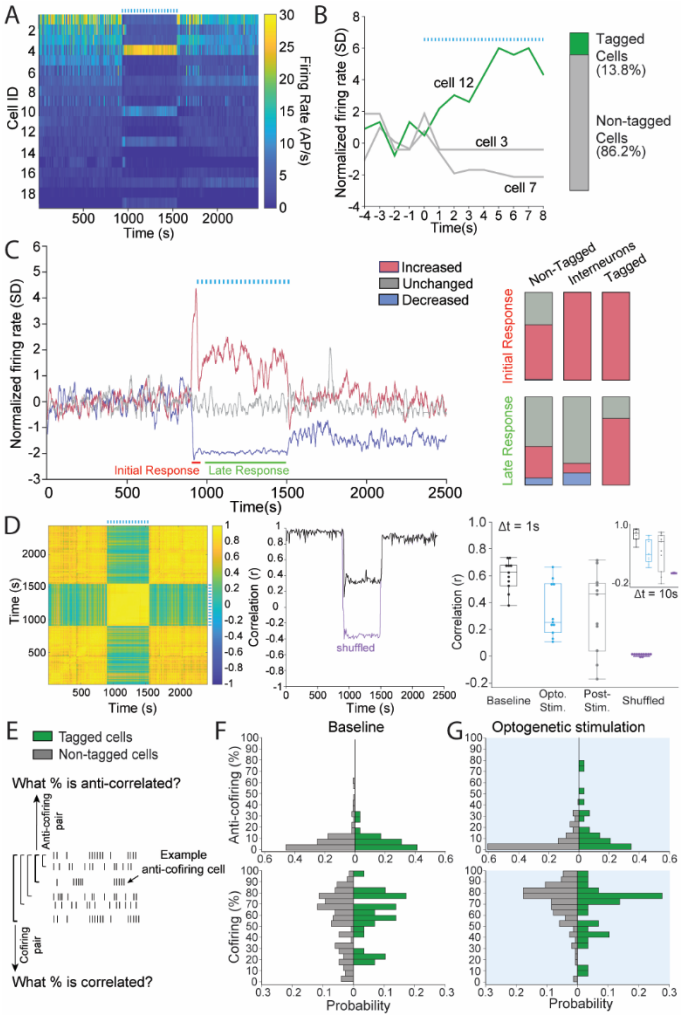

Figure 2. Optogenetic stimulation elicits complex, endogenous patterns of CA1 discharge in the awake behaving mouse. A) 10-s ensemble activity vectors before, during and after 10-Hz light stimulation. B) The baseline and response of 3 example cells. C) (left) 3 cells illustrate

diverse and dynamic responses to photostimulation, (right) prevalence of initial and steady response types characterized according to cell class. D) Example (left) correlation matrix characterizing similarity of 10-s ensemble activity vectors before, during and after photostimulation. Quantification of the similarity to baseline activity in the example (middle) and the summary statistics (right). E) All pair-wise spike train Kendall correlations were computed (left) to estimate ensemble co-firing relationships. The percentage of pairs in which a particular cell was significantly negatively correlated ("anti-cofiring") or positively correlated ("cofiring") was determined for each cell. Histograms show the likelihood that cells participate in (upper) anti-cofiring and (lower) cofiring pairs (F) before and (G) during photostimulation.

The response to photostimulation appeared more complex in drug-free behaving mice; some cells increased or decreased firing, while others were indifferent to stimulation (Fig. 2A). Mice received either 4-Hz (n = 5) or 10-Hz (n = 5) stimulation, with similar effects; 13.8% percent of cells reliably increased firing above baseline within 15 ms of initiating photostimulation (Fig. 2B). Firing was elevated in 100% of this "optotagged" (tagged) subset during the first 30 seconds of photostimulation. During the next 9 minutes of photostimulation the elevated subset decreased significantly to 75.9% (24.1% were unchanged from baseline; test of proportions z = 3.03, p=0.004; Fig. 2C). All putative interneurons increased their firing during the first 30 seconds of photostimulation, but only 11% maintained the increased firing rate throughout the remaining 9 minutes of photostimulation (test of proportions z = 3.05, p = 0.004); 10.7% increased and 14.3% decreased firing, demonstrating diverse network effects of the excitatory stimulation. Most (86.2%) principal cells were not tagged, and of these, 38.8% did not change firing, 61.8% increased and 1.3% decreased firing during the first 30 seconds. During the next 9 minutes of photostimulation 56.2% of the untagged population did not change their firing with respect to baseline, 35.9% increased it, and 7.8% decreased it, further documenting network effects of the photostimulation. The overall pattern of network discharge assessed as 10-s ensemble activity

vectors was 55% correlated to baseline vectors, significantly greater than chance (1%; Fig. 2D; t_{20} = 23.09, $p < 0.0001$), although less than the activity patterns before but not after photostimulation ($F_{2,30}$ = 5.93, p = 0.007; Tukey tests compared to Before: Before > After = During). These observations were similar for 1-s activity vectors (Fig. 2D inset) and confirm the effect of optogenetic stimulation initially appears causal but becomes homeostatic or at least modest within a minute; instead of persistently controlling network discharge, there is a complex steady-state network response. Subsequent analyses focused on the last 9 min of stimulation to estimate the steady-state effect of stimulation.

We next examined the cell-pair cofiring (τ) statistics at 1-s time resolution (Fig. 2E) to estimate the network response (Schneidman et al., 2006; Levy et al., 2021). Of the baseline cofiring relationships, 9% were significantly negative ("anti-cofiring pairs") and 70% were significantly positively ("cofiring pairs"). The individual CA1 cells that have many anti-cofiring relationships with other cells are crucial for discriminating environmental representations [13], which is why we examined whether the tagged and non-tagged cells differed in their likelihood to be in an anti-cofiring relationship. The tagged and non-tagged cells did not differ at baseline (Fig. 2F; t_{181} = 0.63, p = 0.3). However, tagged cells were more likely to be anti-cofiring with other cells during photostimulation (Fig. 2G; t_{181} = 2.28, p = 0.03). Correspondingly, tagged cells were less likely than non-tagged cells to be cofiring with other cells during photostimulation (t_{181} = 1.86, p = 0.03).

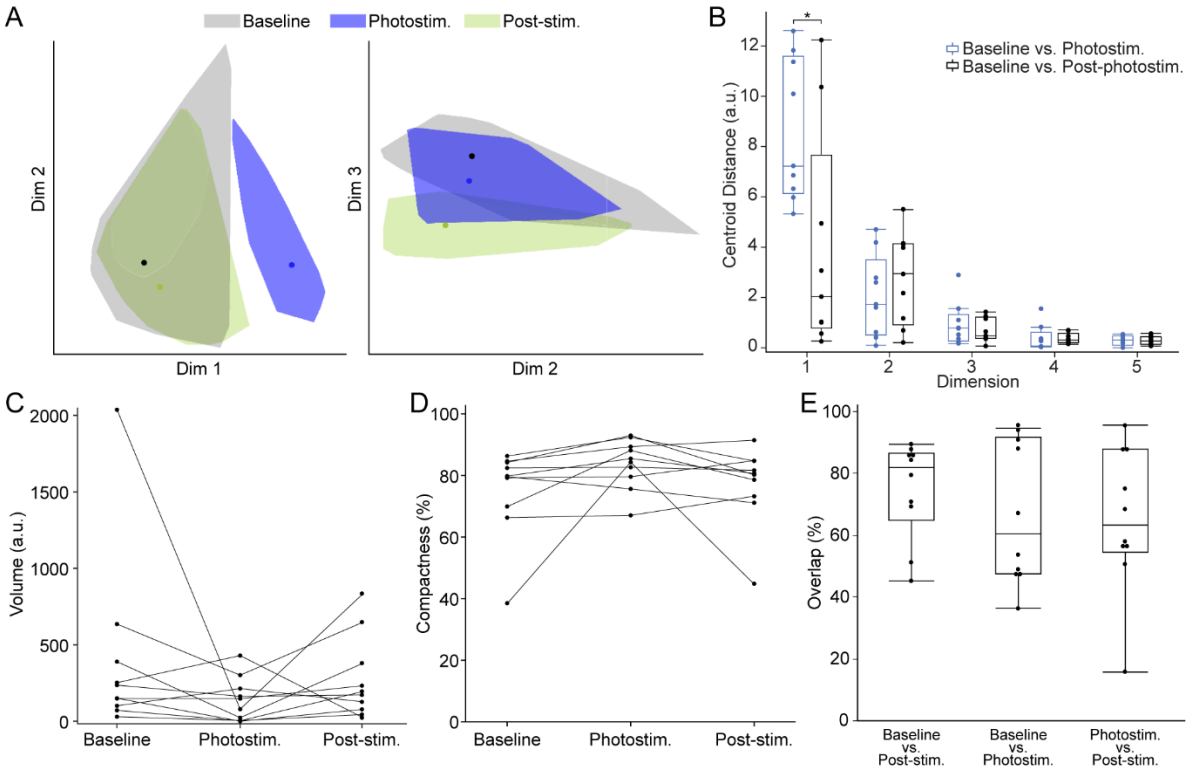

Figure 3. Optogenetic stimulation does not change the low-dimensional geometry of CA1 population discharge. A) 3-D Isomap projections of an example 25-cell cluster recording before, during and after photostimulation, from two points of view. Differences between the projections from ten recordings B) summarized as the distances between the projection centroids in the primary five dimensions, and further quantified by measures of C) volume, D) compactness (radius containing 90% of samples), and E) centroid-aligned overlap (inset: cartoon of the measurement).

Because 15-20% of the most anti-cofiring subpopulation of CA1 cells is responsible for distinguishing manifold environmental representations [13], we projected the 1-s neural activity vectors into a 3-D subspace using the non-linear IsoMap dimensionality reduction algorithm [14]. Baseline and photostimulated manifold projections were remarkably similar. The centroids of photostimulated activity only differed from baseline more than post-stimulated activity differed

from baseline in the primary dimension (Fig. 3A,B) and the geometric differences were not greater than the differences between the pre- and post-stimulation population patterns according to multiple additional measures (Fig. 3C-E). These findings indicate that the optogenetic stimulation was not sufficient to qualitatively change neural activity, consistent with homeostatic hypotheses and evidence [15].

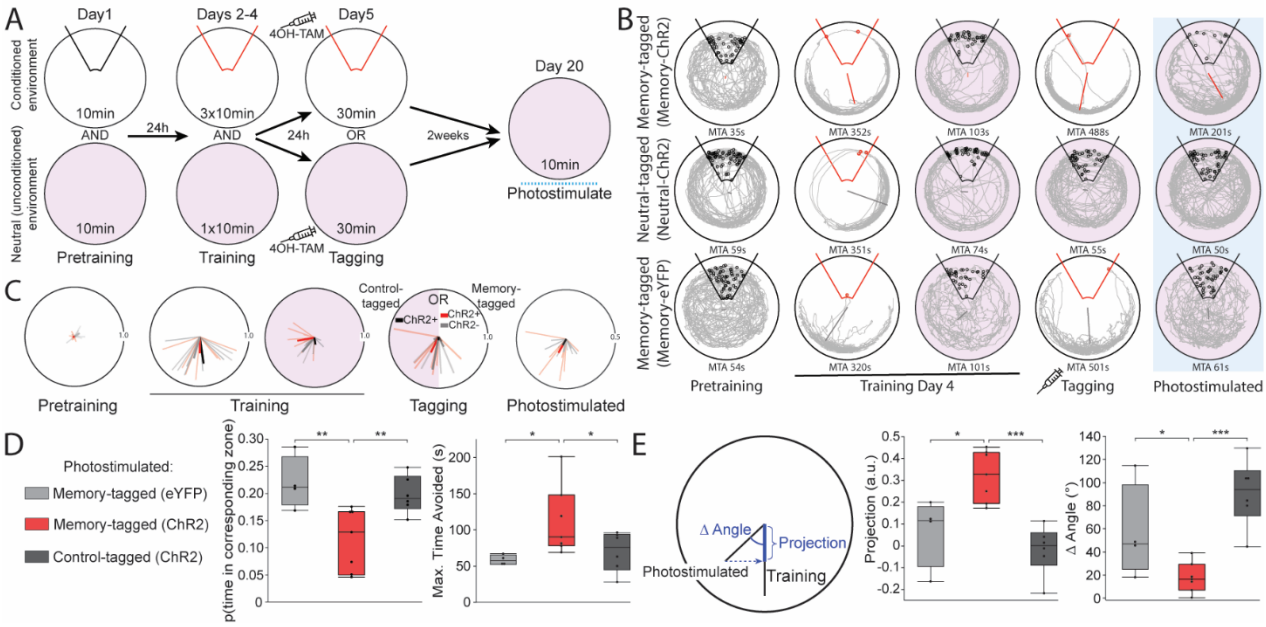

Figure 4. Optogenetic stimulation elicits conditioned active place avoidance behavior in the unconditioned environment, despite never experiencing shock there. A) Experimental design. B) Tracks of three exemplar mice in the conditioned and unconditioned environments during select behavioral trials. Each resultant vector overlay indicates the preferred polar location. C) Distribution of resultant vectors across the behavioral protocol. Color-code as in panel D. Avoiding the location in the unconditioned environment that corresponds to the shock zone in the conditioned environment quantified as D) the probability of being in zone (left) and MTA, the maximum time of avoiding the zone (right). E) The similarity of the photostimulated avoidance to the shock-elicited avoidance was quantified by the projection of the light-elicited resultant vector onto the training-elicited resultant vector (left) and summarized for each group by the distributions of the projection length (middle) and angle (right). *p<0.05, **p<0.01, ***p<0.001.

Is the CA1 network's relative indifference to the photostimulation a property of a complex system [7], or is it simply because the stimulation was insufficient to be consequential (Fig. 1,3)? To decide between these alternatives, we examined whether the optogenetic stimulation was sufficient to elicit the conditioned active place avoidance behavior in an environment where the mice do not express an avoidance. As before, mice received 10 minutes of active place avoidance training three times a day for four days in one environment. Each day, before or after one of the place avoidance trials, the mice were put for 10 minutes in a neutral environment that was identical except that transparent plastic covered the floor, the ambient scent was different, and shock was never on (Fig. 4A). After four days of training the mice did not express an avoidance in the neutral environment and Arc-CreER^{T2}-eYFP-ChR2 experimental mice and Arc-CreER^{T2}-eYFP control mice received 4OH-Tamoxifen (TAM) to tag active neurons. Seven "memory-ChR2" mice and four Arc-CreER^{T2}-eYFP "memory-eYFP" mice received TAM before being put in the place avoidance environment. Six Arc-CreER^{T2}-eYFP-ChR2 "neutral-ChR2" mice received TAM before being put in the neutral environment. Two weeks later, all mice were returned to the neutral environment with 473-nm photostimulation at either 4-Hz (n = 8) or 10-Hz (n = 9) with similar effects. Whereas memory-eYFP and neutral-ChR2 mice walked throughout the neutral environment, memory-ChR2 mice tended to avoid the area corresponding to the shock zone (Fig. 4B), which could be described for each mouse by the Rayleigh vector of the dwell angles within the circular environment (Fig. 4C), as well as thigmotaxis that is characteristic of training sessions. We quantified the avoidance by the probability of being in the corresponding shock zone, analyzed in two 5-min epochs. The probability was decreased in the memory-ChR2 mice (Fig. 4D; $F_{2,27.8} = 10.3$, $p = 0.0005$), and increased in the second epoch ($F_{1,27.8} = 5.3$, $p = 0.03$), with no group X epoch interaction ($F_{2,27.8} = 0.44$, $p = 0.6$; Tukey tests: memory-ChR2 < neutral-ChR2 = memory-eYFP). Similarly, the memory-ChR2 mice avoided the zone for longer periods of time than the neutral-ChR2 and memory-eYFP mice (Fig. 4D; $F_{2,26.6} = 6.8$, $p = 0.004$; Tukey tests:

memory-ChR2 > neutral-ChR2 = memory-eYFP). Neither the effects of epoch nor the group X epoch interaction were significant (F's ≤ 0.9, p's ≥ 0.3). These group differences were not due to the mice walking at different speeds ($F_{2,28}$ = 1.7, p = 0.2).

Because each mouse's place avoidance was unique in the conditioned environment, we characterized the avoidance during the last place avoidance training session on day 5 with the Rayleigh vector of all the mouse's angular positions. These tended to be long and idiosyncratically oriented away from the shock zone for avoidance training sessions and short for corresponding sessions on the neutral environment (Fig. 4C). If photostimulation in the neutral environment causes the mice to express their particular avoidance, then each mouse's Rayleigh vector during photostimulation in the neutral environment should resemble the mouse's Rayleigh vector during the last training session. As predicted, the length of the projection of the "photostimulation" vector onto the "training" vector was longest in the memory-ChR2 group (Fig. 4E; $F_{2,14}$ = 12.74, p = 0.001, Tukey tests: memory-ChR2 > neutral-ChR2 = memory-eYFP). The angular difference between the photostimulation and training vectors were also smallest in the memory-ChR2 group (Fig. 4E; $F_{2,14}$ = 11.96, p = 0.001, Tukey tests: memory-ChR2 < memory-eYFP = neutral-ChR2). These findings provide compelling evidence that the photostimulation of memory-ChR2 mice in the neutral environment was sufficient to elicit the specific learned avoidance that had been tagged during the last training session before photostimulation.

Photostimulating a subset of active place avoidance memory-tagged cells is sufficient to elicit behavioral expression of the memory in a familiar neutral environment, yet the same stimulation did not elicit novel patterns of neural discharge in the hippocampus output (see Video S1 for photostimulation that elicits the conditioned avoidance in a memory-ChR2 mouse but not a neutral-ChR2 mouse, in a completely novel environment). Memory-tagging as performed here was driven by *Arc* activation that only captures a subset of memory-activated cells that likely only

weakly overlap with cells that activate immediate early genes *cFos* and *Npas4* that are each sufficient to identify hippocampal cells that are crucial for an aversive memory [12,16]. Although their activity is sufficient for eliciting the conditioned response, it is unclear whether the memory-tagged cells are the most Arc-activated and/or the most electrophysiologically active subpopulation [17,18]. Our experimental design extends the "engram cell" reactivation phenomenon from non-spatial threat avoidance conditioning [19,20], demonstrating that optogenetic tagging and stimulation is also effective for an active place avoidance memory that is exquisitely sensitive to hippocampal function [21,22] and dependent on the months-long persistence of PKMζ-maintained long-term potentiation in hippocampus [11,23,24]. As is the case for threat avoidance memories, we expect that active place avoidance memories activate neurons across distributed brain regions, not just hippocampus [25]. Engram cell activation experiments tend to photostimulate for 3-6 minutes. We observed that after an initial, transient activation lasting < 30 s, the CA1 network adapts to continued photostimulation (Fig. 2,3), consistent with homeostatic hypotheses and incompatible with causal hypotheses. Prudence is thus warranted when interpreting the results of experimental designs that intend causal manipulations of neural circuits in awake, behaving animals, because the manipulations elicit homeostatic, endogenous patterns of activity rather than stimulus-triggered responses that can be observed under anesthesia, which may compromise excitation-inhibition coordination Fig. 1; [26]. While feedforward conceptions of neural circuits predict linear responses to tagged-neuron photostimulation as demonstrated in reduced preparations [27], we demonstrate substantially invariant network responses despite single neuron activity changes, as expected if feedback, recurrence, inhibition, and other neural connectivity motifs provide for complex system dynamics (Fig. 1). While these motifs include and depend upon synaptic function, some engram cell experiments have been interpreted to indicate that modified synaptic function has no role in memory storage, which is at odds with the present findings [28,29]. We conclude that unless neural activity is measured directly, the outcomes of engram-cell, behavioral timescale synaptic plasticity, and similar neural system manipulations should be parsimoniously interpreted

as the expression of the homeostatic, endogenous population dynamics of a complex system, rather than the precise causal responses of a neural circuit.

REFERENCES

1 Stark, E., Roux, L., Eichler, R. & Buzsaki, G. Local generation of multineuronal spike sequences in the hippocampal CA1 region. *Proc Natl Acad Sci U S A* **112**, 10521-10526, doi:10.1073/pnas.1508785112 (2015).

2 Dragoi, G. & Tonegawa, S. Distinct preplay of multiple novel spatial experiences in the rat. *Proc Natl Acad Sci U S A* **110**, 9100-9105, doi:1306031110 [pii] 10.1073/pnas.1306031110 (2013).

3 Vyas, S., Golub, M. D., Sussillo, D. & Shenoy, K. V. Computation Through Neural Population Dynamics. *Annual Review of Neuroscience* **43**, 249-275, doi:10.1146/annurev-neuro-092619-094115 (2020).

4 Park, E. H., Keeley, S., Savin, C., Ranck, J. B., Jr. & Fenton, A. A. How the Internally Organized Direction Sense Is Used to Navigate. *Neuron* **101**, 1-9, doi:10.1016/j.neuron.2018.11.019 (2019).

5 Dubreuil, A., Valente, A., Beiran, M., Mastrogiuseppe, F. & Ostojic, S. The role of population structure in computations through neural dynamics. *Nature Neuroscience* **25**, 783-794, doi:10.1038/s41593-022-01088-4 (2022).

6 Rogers, S., Rozman, P. A., Valero, M., Doyle, W. K. & Buzsaki, G. Mechanisms and plasticity of chemogenically induced interneuronal suppression of principal cells. *Proc Natl Acad Sci U S A* **118**, doi:10.1073/pnas.2014157118 (2021).

7 Ashby, W. R. Requisite variety and its implications for the control of complex systems. *Cybernetica* **1**, 83-99 (1958).

8 Tonegawa, S., Liu, X., Ramirez, S. & Redondo, R. Memory Engram Cells Have Come of Age. *Neuron* **87**, 918-931, doi:10.1016/j.neuron.2015.08.002 (2015).

9 Bittner, K. C. *et al.* Conjunctive input processing drives feature selectivity in hippocampal CA1 neurons. *Nat Neurosci* **18**, 1133-1142, doi:10.1038/nn.4062 (2015).

10 Vazdarjanova, A. *et al.* Spatial exploration induces ARC, a plasticity-related immediate-early gene, only in calcium/calmodulin-dependent protein kinase II-positive principal excitatory and inhibitory neurons of the rat forebrain. *J Comp Neurol* **498**, 317-329, doi:10.1002/cne.21003 (2006).

11 Hsieh, C. *et al.* Persistent increases of PKMzeta in memory-activated neurons trace LTP maintenance during spatial long-term memory storage. *Eur J Neurosci* **54**, 6795-6814, doi:10.1111/ejn.15137 (2021).

12 Denny, C. A. *et al.* Hippocampal memory traces are differentially modulated by experience, time, and adult neurogenesis. *Neuron* **83**, 189-201, doi:S0896-6273(14)00404-8 [pii] 10.1016/j.neuron.2014.05.018 (2014).

13 Levy, E. R. J. *et al.* A manifold neural population code for space in hippocampal coactivity dynamics independent of place fields. *bioRxiv*, 2021.2007.2026.453856, doi:10.1101/2021.07.26.453856 (2021).

14 Balasubramanian, M. & Schwartz, E. L. The isomap algorithm and topological stability. *Science* **295**, 7, doi:10.1126/science.295.5552.7a (2002).

15 McKenzie, S. *et al.* Preexisting hippocampal network dynamics constrain optogenetically induced place fields. *Neuron* **109**, 1040-1054 e1047, doi:10.1016/j.neuron.2021.01.011 (2021).

16 Sun, X. *et al.* Functionally Distinct Neuronal Ensembles within the Memory Engram. *Cell* **181**, 410-423 e417, doi:10.1016/j.cell.2020.02.055 (2020).
17 Guzowski, J. F. *et al.* Recent behavioral history modifies coupling between cell activity and Arc gene transcription in hippocampal CA1 neurons. *Proc Natl Acad Sci U S A* **103**, 1077-1082, doi:0505519103 [pii]
10.1073/pnas.0505519103 (2006).
18 Mizuseki, K. & Buzsaki, G. Preconfigured, skewed distribution of firing rates in the hippocampus and entorhinal cortex. *Cell Rep* **4**, 1010-1021, doi:S2211-1247(13)00401-4 [pii]
10.1016/j.celrep.2013.07.039 (2013).
19 Ramirez, S. *et al.* Creating a false memory in the hippocampus. *Science* **341**, 387-391, doi:341/6144/387 [pii]
10.1126/science.1239073 (2013).
20 Garner, A. R. *et al.* Generation of a synthetic memory trace. *Science* **335**, 1513-1516, doi:335/6075/1513 [pii]
10.1126/science.1214985 (2012).
21 Cimadevilla, J. M., Fenton, A. A. & Bures, J. Functional inactivation of dorsal hippocampus impairs active place avoidance in rats. *Neurosci Lett* **285**, 53-56, doi:S0304-3940(00)01019-3 [pii] (2000).
22 Cimadevilla, J. M., Wesierska, M., Fenton, A. A. & Bures, J. Inactivating one hippocampus impairs avoidance of a stable room-defined place during dissociation of arena cues from room cues by rotation of the arena. *Proc Natl Acad Sci U S A* **98**, 3531-3536, doi:10.1073/pnas.051628398
98/6/3531 [pii] (2001).
23 Pastalkova, E. *et al.* Storage of spatial information by the maintenance mechanism of LTP. *Science* **313**, 1141-1144, doi:10.1126/science.1128657 (2006).
24 Pavlowsky, A., Wallace, E., Fenton, A. A. & Alarcon, J. M. Persistent modifications of hippocampal synaptic function during remote spatial memory. *Neurobiol Learn Mem* **138**, 182-197, doi:10.1016/j.nlm.2016.08.015 (2017).
25 Roy, D. S. *et al.* Brain-wide mapping reveals that engrams for a single memory are distributed across multiple brain regions. *Nat Commun* **13**, 1799, doi:10.1038/s41467-022-29384-4 (2022).
26 Chung, A. *et al.* Cognitive control persistently enhances hippocampal information processing. *Nature* **600**, 484-488, doi:10.1038/s41586-021-04070-5 (2021).
27 Boyden, E. S., Zhang, F., Bamberg, E., Nagel, G. & Deisseroth, K. Millisecond-timescale, genetically targeted optical control of neural activity. *Nat Neurosci* **8**, 1263-1268, doi:10.1038/nn1525 (2005).
28 Ryan, T. J., Roy, D. S., Pignatelli, M., Arons, A. & Tonegawa, S. Memory. Engram cells retain memory under retrograde amnesia. *Science* **348**, 1007-1013, doi:10.1126/science.aaa5542 (2015).
29 Tonegawa, S., Pignatelli, M., Roy, D. S. & Ryan, T. J. Memory engram storage and retrieval. *Curr Opin Neurobiol* **35**, 101-109, doi:10.1016/j.conb.2015.07.009 (2015).